Mineralogical Magazine, October 2016, Vol. 80(6), pp. 985–994

Albertiniite, $Fe^{2+}(SO_3)\cdot 3H_2O$, a new sulfite mineral species from the Monte Falò Pb-Zn mine, Coiromonte, Armeno Municipality, Verbano Cusio Ossola Province, Piedmont, Italy

P. Vignola[1,2,*], G. D. Gatta[2], N. Rotiroti[2], P. Gentile[3], F. Hatert[4], M. Baijot[4], D. Bersani[5], A. Risplendente[2] and A. Pavese[2]

[1] CNR-Istituto per la Dinamica dei Processi Ambientali, via Botticelli 23, I-20133, Milano, Italy.
[2] Dipartimento di Scienze della Terra "A. Desio", Università degli Studi di Milano, via Botticelli 23, I-20133 Milano, Italy.
[3] Dipartimento di Scienze dell'Ambiente e del Territorio e di Scienze della Terra, Università Milano-Bicocca, Piazzale della Scienza 4-building U4, I-20126 Milano, Italy.
[4] Laboratoire de Minéralogie, Département de Géologie, Université de Liège, Bâtiment B18, Sart Tilman, B-4000 Liège, Belgium.
[5] Dipartimento di Fisica e Scienze della Terra, Università di Parma, Viale G.P. Usberti 7/a, I-43124 Parma, Italy

[*Received 19 July 2015; Accepted 13 September 2015; Associate Editor: Stuart Mills*]

ABSTRACT

Albertiniite, $Fe^{2+}(SO_3)\cdot 3H_2O$, is a new Fe^{2+} sulfite trihydrate, related chemically to gravegliaite. It occurs at the Monte Falò Pb-Zn mine near Coiromonte, in the Armeno Municipality, Verbano–Cusio–Ossola Province, Italy. It is an intermediate product of oxidation between iron sulfides and sulfates, forming monoclinic, colourless to pale yellow, transparent crystals with a vitreous lustre. The mineral occurs associated with stolzite, pyromorphite, hinsdalite, plumbogummite, gibbsite, scheelite and jarosite on brittle fractures of quartz veins or chlorite-schist. Albertiniite is optically biaxial (+) with $2V_{(meas)} \approx 40°$ and $2V_{(calc)} = 66°$. The measured refractive indices, using sodium light (589 nm) are: $\alpha = 1.612(2)°$, $\beta = 1.618(2)°$ and $\gamma = 1.632(2)°$. The optical axis plane is parallel to the perfect {010} cleavage plane. It is non-fluorescent under shortwave (254 nm) or longwave (366 nm) ultraviolet light. The calculated density is 2.469 g cm^{-3} (from the crystal-structure refinement), or 2.458 g cm^{-3} (from the chemical analysis and the single-crystal unit-cell parameters). The empirical formula is (average of 16 spots and based on 3 anhydrous oxygen apfu) $(Fe^{2+}_{0.774}Mn^{2+}_{0.282}Ca_{0.001}Mg_{0.001}Na_{0.003})_{\sum 1.061}(S_{0.971}O_3)\cdot 2.84H_2O$, with the H_2O content calculated by difference to 100 wt.%. Albertiniite is monoclinic, with space group $P2_1/n$. Its unit-cell parameters are: $a = 6.633(1)$, $b = 8.831(1)$, $c = 8.773(1)$ Å, $\beta = 96.106(8)°$ and $V = 511.0(1)$ Å^3,with $Z = 4$. The eight strongest measured lines in the powder X-ray diffraction pattern are [d in Å, (I/I_0), (hkl)]: 4.072 (100) ($\bar{1}11$), 3.539 (93) ($\bar{1}12$), 5.533 (27) ($\bar{1}01$), 6.167 (14) (011), 2.830 (14) (211), 4.998 (14) (101), 4.353 (12) (111) and 3.897 (12) (012). The mineral, which has been approved by the CNMNC, number IMA2015-004, is named albertiniite in honour of Claudio Albertini, an Italian mineral collector and expert in the systematic mineralogy of the Alps and pegmatites.

Keywords: albertiniite, Fe sulfite trihydrate, Monte Falò Pb-Zn mine, Verbania province, Italy, new mineral.

Introduction

Mineral species belonging to the sulfite subgroup, oxide class in the classification of Strunz (Strunz and Nickel, 2001), are very rare in nature. The four known species belonging to this subgroup are gravegliaite, $Mn^{2+}(SO_3)\cdot 3H_2O$, hannebachite, $Ca(SO_3)\cdot H_2O$, scotlandite, $Pb(SO_3)$ and the sulfate-sulfite orschallite, $Ca_3(SO_3)_2(SO_4)\cdot 12H_2O$. Gravegliaite and scotlandite can be considered as intermediate products of the oxidation process which transforms oxides and sulfides into sulfates, where

*E-mail pietro.vignola@idpa.cnr.it
DOI: 10.1180/minmag.2016.080.033

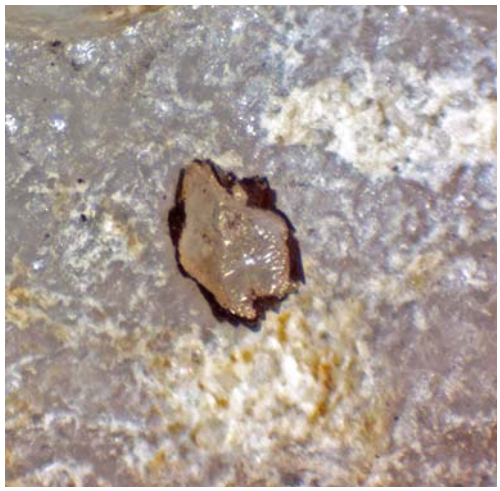

FIG. 1. Albertiniite, crystal 0.4 mm × 0.25 mm from Monte Falò. Co-type specimen at the Museum of Natural History of Milano (catalogue number 38728).

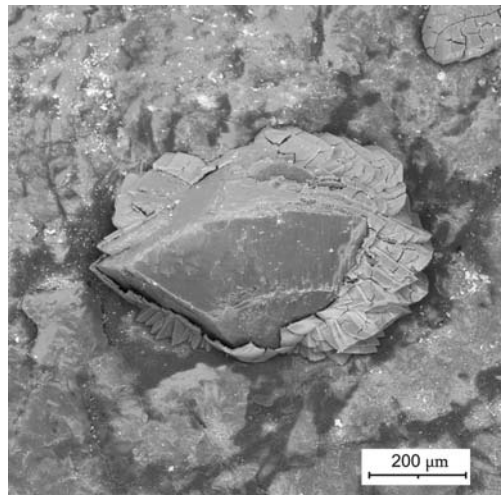

FIG. 2. Back-scattered electron image of albertiniite from Monte Falò.

hannebachite and orschallite crystallize in a moderately oxidizing hydrothermal environment. Hannebachite and orschallite were found and described for the first time in the magmatic rocks of the Eifel volcanic area (Palatinate, Germany) (Hentschel *et al.*, 1985; Weidenthaler *et al.*, 1993). Scotlandite, more common in respect of the other three species, was described for the first time at the Susanna lead mine, Leadhills, Scotland (Paar *et al.*, 1984), as a product of oxidation of galena and Pb-sulfides. Gravegliaite was described as the product of oxidation of the braunite + hausmannite + tephroite mineralization at the Gambatesa Mn mine, Val Graveglia, Italy, as micro-crystals along fractures in the Mn mineralization (Basso *et al.*, 1991). Albertiniite is an iron sulfite trihydrate, related chemically to gravegliaite. The mineral and its name has been approved by the IMA Commission on New Minerals, Nomenclature and Classification (IMA2015-004, Vignola *et al.*, 2015). The mineral is named in honour of Claudio Albertini, an Italian mineral collector and expert in the systematic mineralogy of the Alps and pegmatites. Claudio Albertini is an author of several papers in the principal journals for mineral collectors and scientists, and he is author of the volume "*L'Alpe Devero e*

TABLE 1 Electron microprobe analysis of albertiniite.

	Wt.%*	SD	Range		apfu**
SO_2	32.88	0.77	(31.54–33.95)	S	0.971
FeO	29.38	1.89	(24.29–32.40)	Fe^{2+}	0.774
MnO	10.58	1.47	(8.60–14.46)	Mn^{2+}	0.282
CaO	0.02	0.01	(0.01–0.04)	Ca	0.001
MgO	0.01	0.02	(0.00–0.08)	Mg	0.001
Na_2O	0.05	0.03	(0.00–0.09)	Na	0.003
H_2O	27.07			OH^-	2.84
Total	100				

*Average of 16 analyses.
**Calculated on the basis of 3 (anhydrous) oxygen apfu with H_2O by difference to 100 wt.%.
SD – standard deviation.

https://doi.org/10.1180/minmag.2016.080.033 Published online by Cambridge University Press

i suoi minerali" on the worldwide famous locality of Mount Cervandone. Claudio found, and proposed to the scientific community, the new mineral species: fetiasite (Graeser *et al.*, 1994), albertiniite (present work) and a new phase still under investigation. Co-type samples used for the complete characterization of the new species albertiniite are deposited in the Mineralogical Collection of the Museo Civico di Storia Naturale, Milano, Italy, (Fig. 1) (number MM 38728; co-type used for chemical analysis, paragenesis description, powder X-ray diffraction, Raman spectroscopy), and in the collection of the Laboratory of Mineralogy, University of Liège, Belgium (number 20393; co-type used for optical measurements and single-crystal X-ray structure determination).

Appearance and physical properties

Albertiniite was found by Claudio Albertini in 2010 on the mine dumps at the Monte Falò Pb-Zn mine near Coiromonte, Armeno Municipality, Verbano-Cusio-Ossola Province, Italy (45°50'52.37″N, 8°29'1.13″E). The mine was active in the period 1920–1953 and the tunnels (now collapsed) reached a total length of ~340 m. Galena was the most important mined mineral, with minor sphalerite, arsenopyrite, pyrite and marcasite (Albertini *et al.*, 2014). The ore is constituted by the aforementioned sulfides hosted by quartz veins embedded in a chlorite-rich micaschist, characterized by an unusual secondary mineral association of stolzite, pyromorphite,

TABLE 2 Powder X-ray diffraction data for albertiniite.

I/I_0	d_{obs}	d_{calc}	h k l
14	6.167	6.205	0 1 1
27	5.533	5.554	$\bar{1}$ 0 1
11	5.257	5.284	1 1 0
14	4.998	5.008	1 0 1
100	4.721	4.702	$\bar{1}$ 1 1
12	4.353	4.356	1 1 1
12	3.897	3.909	0 1 2
93	3.539	3.515	$\bar{1}$ 1 2
10	3.29	3.297	2 0 0
10	3.076	3.089	2 1 0
9	2.994	3.008	$\bar{2}$ 1 1
7	2.873	2.894	$\bar{1}$ 2 2
14	2.83	2.824	2 1 1
8	2.759	2.761	0 1 3
4	2.23	2.232	$\bar{2}$ 1 3
4	2.183	2.18	0 0 4
4	2.169	2.166	$\bar{2}$ 3 1
6	2.115	2.116	0 1 4
5	2.022	2.02	1 4 1
3	2.003	2	$\bar{3}$ 1 2
3	1.912	1.913	$\bar{1}$ 4 2
4	1.873	1.872	$\bar{2}$ 1 4
3	1.862	1.863	1 4 2
2	1.819	1.817	$\bar{2}$ 4 1
2	1.665	1.666	1 5 1
3	1.416	1.416	$\bar{2}$ 3 5
2	1.413	1.412	4 2 2

The strongest lines are given in bold.

TABLE 3 Details of the single-crystal X-ray data collection and structure refinement of albertiniite.

Crystal shape	Irregular prism
Crystal size (mm^3)	0.180 × 0.150 × 0.090
Crystal colour	Transparent, colourless
T (K)	298
Unit-cell constants	a = 6.633 (1) Å
	b = 8.831 (1) Å
	c = 8.773 (1) Å
	β = 96.106 (8)°
	V = 511.0 (1) $Å^3$
Reference chemical formula	$Fe^{2+}(SO_3)\cdot 3H_2O$
Space Group	$P2_1/n$
Z	4
Radiation (Å)	Mo$K\alpha$
Diffractometer	Xcalibur – CCD
Data-collection method	ω/φ scan
Step size (°) / Time per frame (s)	1 / 10
Max. θ (°)	72.33
	$-8 < h < 8$
	$-14 < k < 14$
	$-13 < l < 14$
No. measured reflections	14,415
No. unique reflections	1668
No. unique refl. with $F_o > 4\sigma(F_o)$	1409
No. refined parameters	92
Refinement on	F^2
R_{int}*	0.0339
R_1 (F) with $F_o > 4\sigma(F_o)$	0.0227
R_1 (F) for all the unique reflections	0.0342
wR_2 (F^2)	0.0429
Goof	1.657
Weighting scheme: a, b	0.01, 0
Residuals (e $Å^{-3}$)	+0.504 / –0.494

*$R_{int} = \Sigma \mid F^2_{obs} - F^2_{obs}$ (mean) $\mid / \Sigma [F^2_{obs}]$; $R_1 = \Sigma(|F_{obs}| - |F_{calc}|)/\Sigma|F_{obs}|$; $wR_2 = [\Sigma[w(F^2_{obs} - F^2_{calc})^2]/\Sigma[w(F^2_{obs})^2]]^{0.5}$, $w = 1/ [\sigma^2(F^2_{obs}) + (a*P)^2 + b*P]$, $P = (\text{Max}(F^2_{obs}, 0) + 2*F^2_{calc})/3$.

https://doi.org/10.1180/minmag.2016.080.033 Published online by Cambridge University Press

TABLE 4 Refined fractional coordinates and displacement parameters (Å^2) in the expression: $-2\pi^2[(ha^*)^2U^{11} + \ldots + 2hka^*b^*U^{12} + \ldots + 2klb^*c^*U^{23}]$. U_{eq} is defined as one third of the trace of the orthogonalized U_{ij} tensor*.

Site	*x*/*a*	*y*/*b*	*z*/*c*	U^{11}	U^{22}	U^{33}	U^{23}	U^{13}	U^{12}	$U_{eq./iso}$
M	0.42944(4)	0.24709(2)	0.14459(2)	0.0124(1)	0.01203(9)	0.01331(11)	0.00146(8)	0.00112(9)	0.00001(9)	0.0126(1)
S	0.82444(6)	0.07021(4)	0.32605(4)	0.0088(1)	0.0135(1)	0.0118(2)	–0.0004(1)	0.0019(1)	–0.0001(1)	0.0113(1)
O1	0.9551(2)	0.1986(1)	0.4052(1)	0.0150(7)	0.0193(5)	0.0151(5)	–0.0058(4)	0.0015(5)	–0.0027(5))	0.0165(2)
O2	0.7224(2)	0.1429(1)	0.1794(1)	0.0142(7)	0.0242(5)	0.0157(5)	–0.0006(4)	–0.0025(5)	0.0074(5)	0.0183(2)
O3	0.5211(2)	0.4623(1)	0.2333(1)	0.0175(7)	0.0124(5)	0.0197(5)	–0.0005(4)	0.0041(5)	–0.0040(4)	0.0164(2)
O4	0.1117(2)	0.3475(1)	0.1431(1)	0.0144(7)	0.0156(5)	0.0183(5)	0.0006(4)	0.0010(5)	–0.0004(5)	0.0161(2)
O5	0.2667(2)	0.0461(1)	0.0742(1)	0.0301(8)	0.0224(6)	0.0177(6)	–0.0066(4)	0.0071(5)	–0.0098(6)	0.0231(3)
O6	0.3613(19)	0.1682(1)	0.3745(1)	0.0127(7)	0.0244(6)	0.0119(5)	0.0013(5)	0.0001(5)	0.0001(5)	0.0164(2)
H1	0.454(3)	0.181(3)	0.461(2)							0.050(3)
H2	0.234(2)	0.174(3)	0.403(2)							0.050(3)
H3	0.270(3)	–0.002(2)	–0.018(1)							0.050(3)
H4	0.157(2)	0.023(2)	0.128(2)							0.050(3)
H5	0.034(3)	0.311(3)	0.216(2)							0.050(3)
H6	0.115(3)	0.453(1)	0.145(2)							0.050(3)

* The *M* site was modelled with the scattering curve of Fe.

TABLE 5 Refined bond distances (Å) and angles (°).

M–O1	2.178(1)	O1–M–O2	93.99(4)
M–O2	2.143(1)	O1–M–O3	96.19(4)
M–O3	2.118(1)	O1–M–O4	94.32(4)
M–O4	2.285(1)	O1–M–O5	89.62(4)
M–O5	2.134(1)	O1–M–O6	170.97(4)
M–O6	2.222(1)	O2–M–O3	96.45(4)
		O2–M–O4	171.66(4)
S–O1	1.546(1)	O2–M–O5	96.16(5)
S–O2	1.529(1)	O2–M–O6	90.00(4)
S–O3	1.530(1)	O3–M–O4	83.25(4)
		O3–M–O5	165.70(5)
O6–H1	0.93(2)	O3–M–O6	91.40(4)
H1···O4	1.83(2)	O4–M–O5	83.29(5)
O6···O4	2.73(1)	O4–M–O6	81.68(4)
O6–H1···O4	164(1)	O5–M–O6	81.89(4)
O6–H2	0.92(1)	O1–S–O2	104.29(6)
H2···O1	1.86(1)	O1–S–O3	104.25(7)
O6···O1	2.76(1)	O2–S–O3	103.14(6)
O6–H2···O1	164(1)		
H1–O6–H2	108(2)		
H3–O5–H4	116(2)		
O5–H3	0.92(2)	O5–H4	0.93(2)
H3···O2	1.89(2)	H4···O3	1.86(2)
O5···O2	2.79(1)	O5···O3	2.78(1)
O5–H3···O2	167(1)	O5–H4···O3	168(2)
H5–O4–H6	110(2)		
O4–H5	0.92(2)	O4–H6	0.93(1)
H5···O1	2.05(2)	H6···O6	1.92(1)
O4···O1	2.93(1)	O4···O6	2.84(1)
O4–H5···O1	161(2)	O4–H6···O6	173(1)

hinsdalite, plumbogummite, gibbsite, scheelite, jarosite and albertiniite (mostly covered by an amorphous hydrated iron oxide). The mineral occurs on the surfaces of brittle fractures in quartz veins and in the chlorite-schist hosting the mineralized quartz veins, in monoclinic prisms up to 0.7 mm across, sometimes showing rounded corners and edges. Albertiniite crystals are covered frequently by brownish amorphous hydrated Fe-oxides, probably pseudomorphs after a mineral with a rhombohedral shape (Fig. 2). The mineral shows, under the polarizing microscope, a perfect {010} cleavage; it is brittle with an irregular fracture. The new species forms colourless to yellowish (under natural light) transparent crystals with a vitreous lustre. It is biaxial (+), with $2V_{(meas)} \approx 40°$ and $2V_{(calc)} = 66°$. The measured refractive indexes, using sodium light (589 nm), are: $\alpha = 1.612(2)°$, $\beta = 1.618(2)°$ and $\gamma = 1.632(2)°$. The optical axis plan is parallel to the perfect {010} cleavage plane. The mineral is colourless and non-pleochroic under polarized light. Due to the scarcity of crystals, the density was not measured. The calculated density is 2.469 g cm^{-3} (from the crystal-structure refinement), or 2.458 g cm^{-3} (from the chemical analysis and the single-crystal unit-cell parameters). The compatibility index is 0.012, if calculated with the density obtained from crystal structure data, or 0.008, if calculated with the density obtained from the chemical data. For the compatibility calculations, we used the K_i constants calculated for oxides by Mandarino (1981).

Chemical data

Preliminary chemical data, along with secondary-electron and back-scattered images of albertiniite,

https://doi.org/10.1180/minmag.2016.080.033 Published online by Cambridge University Press

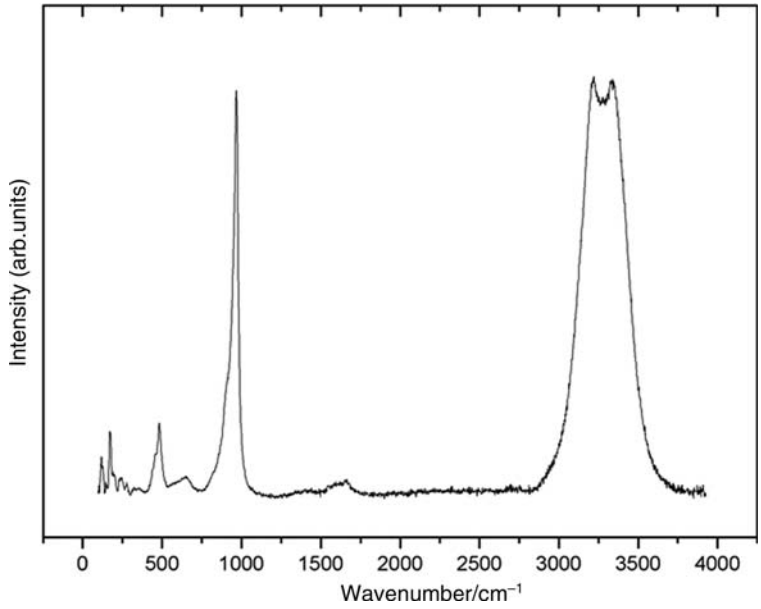

FIG. 3. Unpolarized Raman spectra of albertiniite.

were collected both on natural samples and polished sections by a Tescan Vega TS 5136 XM scanning electron microscope (SEM) equipped with an EDAX Genesis 4000 JXM energy dispersive spectrometer (EDS), at the "Centro interdipartimentale di microscopia elettronica" of the University of Milano-Bicocca. Quantitative chemical analyses were then performed on the polished sections using a JEOL JXA-8200 electron microprobe in wavelength-dispersive mode at the

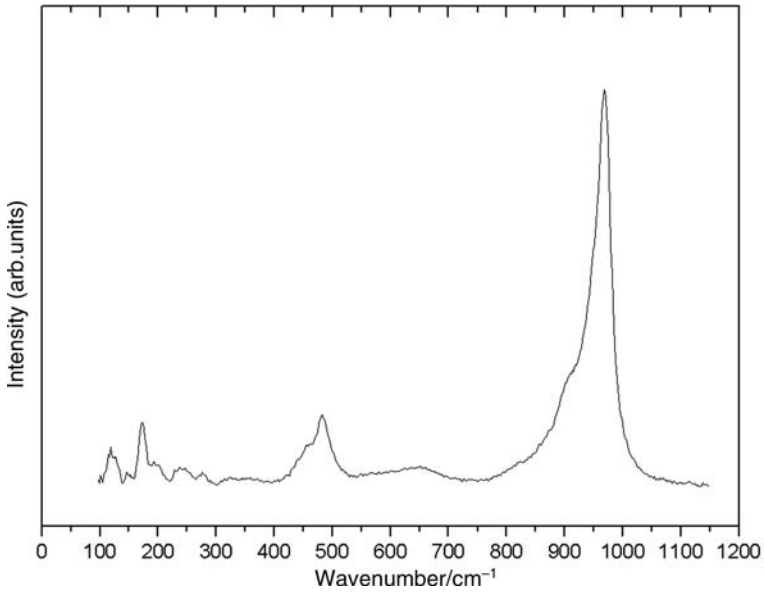

FIG. 4. Unpolarized Raman spectra of albertiniite from 100 to 1100 cm^{-1}.

https://doi.org/10.1180/minmag.2016.080.033 Published online by Cambridge University Press

laboratory of the Earth Sciences Department, University of Milano (ESD-MI). The system was operated using an accelerating voltage of 15 kV, a beam current of 5 nA, a spot size of 15 μm and a counting time of 30 s on the peaks and 10 s on the background. Grossular for Si (*K*α) and Ca (*K*α), celestine for S (*K*α), omphacite for Na (*K*α), fajalite for Fe (*K*α), rhodonite for Mn (*K*α), forsterite for Mg (*K*α), K-feldspar for K (*K*α), graftonite for P (*K*α), realgar for As (*L*α) and cancrinite for Cl (*K*α) served as standards. The raw data were corrected for matrix effects using the ϕρZ method from the JEOL series of programs. The elements Si, P, Al, K and Cl were below detection limits in all 16 microprobe spots. Mean analytical results are reported in Table 1. Due to the small amount of material H_2O was not determined directly but was calculated by difference to 100 wt.%. The empirical formula calculated on the basis of 3 anhydrous oxygen atoms per formula unit (apfu) is $(Fe^{2+}_{0.774}Mn^{2+}_{0.282}Ca_{0.001}Mg_{0.001}Na_{0.003})_{\sum 1.061}(S_{0.971}O_3)\cdot 2.84H_2O$. The simplified formula is $Fe^{2+}(SO_3)\cdot 3H_2O$, which requires SO_2 = 33.73 wt.%, FeO = 37.82 wt.% and H_2O = 28.45 wt.% for a total of 100.00 wt.%.

X-ray diffraction data and crystal structure refinement

The powder X-ray diffraction (PXRD) pattern of albertiniite was collected by a high-resolution Panalytical X'pert Pro X-ray powder diffractometer equipped with a X'Celerator-type detector at the ESD-MI. Operating conditions were: Ni-filtered Cu*K*α radiation, 40 kV, 40 mA, 2θ-range from 5° to 120°, step size of 2θ = 0.017° and a counting time of 300 s per step. Refinement of unit-cell parameters was performed using the program *CELREF 3* (Laugier and Bochu, 1999), based on the structure model obtained by single-crystal X-ray diffraction (see below). Silicon NIST 640c was used as a line-position internal standard. Reflection conditions were found to be consistent with the space group $P2_1/n$. The refined unit-cell parameters are a = 6.633 (10), b = 8.831(9), c = 8.771(13) Å, β = 96.2(2)° and V = 511(1) Å^3 (with Z = 4). The complete list of indexed reflections is reported in Table 2. The eight strongest measured lines are [d in Å, (I/I_0), (hkl)]: 4.072 (100) ($\bar{1}11$), 3.539 (93) ($\bar{1}12$), 5.533 (27) ($\bar{1}01$), 6.167 (14) (011), 2.830 (14) (211), 4.998 (14) (101), 4.353 (12) (111) and 3.897 (12) (012).

Single-crystal X-ray diffraction data were collected with an Xcalibur – Oxford Diffraction diffractometer equipped with a charge-coupled detector (CCD), using graphite-monocromatized Mo*K*α radiation and operated at 50 kV and 40 mA at the ESD-MI. To maximize the reciprocal space coverage, a combination of ω and ϕ scans was used, with a step size of 1° and an exposure time per frame of 10 s. A total number of 14,415 reflections up to $2\theta_{max}$ of 72.3° was collected, out of which 1668 were unique, giving a metrically monoclinic unit cell with: a = 6.633(1), b = 8.831 (1), c = 8.773(1) Å, β = 96.106(8)° and V = 511.0 (1) Å^3 (Table 3). The reflection conditions suggested the space group $P2_1/n$ as highly likely.

X-ray intensity data were first processed with the *E-STATISTICS* programs, implemented in the *WinGX* package (Farrugia, 1999). The statistics of distributions of the normalized structure factors showed, unambiguously (~70% likelihood), that the structure is centrosymmetric. The anisotropic structure refinement was then performed in the space group $P2_1/n$ using the *SHELX-97* software (Sheldrick 1997, 2008), starting from the site coordinates of synthetic α-$Fe^{2+}(SO_3)\cdot 3H_2O$ reported by Johansson and Lindqvist (1979), in which the H sites were not located. Neutral X-ray

TABLE 6 Raman bands measured in albertiniite and their assignments.

Wavenumber (cm^{-1})	Intensity	Assignment
123	m	Lattice mode
172		Lattice mode
197	w	Lattice mode
241	w	Lattice mode
279	w	Lattice mode
324	w,b	Lattice mode
438	w,sh	ν_4 SO_3 (asymmetric bending)
457	m	ν_4 SO_3 (asymmetric bending)
482	m	ν_4 SO_3 (asymmetric bending)
495	sh	ν_4 SO_3 (asymmetric bending)
600	w,b	ν_2 SO_3 (symmetric bending)
660	w,b	ν_2 SO_3 (symmetric bending)
825	w	ν_3 SO_3 (asymmetric stretching)
860	w	ν_3 SO_3 (asymmetric stretching)
910	m	ν_3 SO_3 (asymmetric stretching)
950	s	ν_3 SO_3 (asymmetric stretching)
970	vs	ν_1 SO_3 (symmetric stretching)
1660	w	O–H–O bending (H_2O)
3215	vs	OH stretching (H_2O)
3350	vs	OH stretching (H_2O)

vs = very strong; s = strong; m = medium; mw = medium weak; w = weak; b = broad; sh = shoulder.

https://doi.org/10.1180/minmag.2016.080.033 Published online by Cambridge University Press

scattering curves for Fe, Mn, S, O and H were used according to the *International Tables for Crystallography C* (Wilson and Prince, 1999). The secondary isotropic extinction effect was modelled according to the Larson's formalism (Larson, 1967), as implemented in the *SHELXL-97* package (Sheldrick 1997, 2008), though the refined value of the extinction coefficient was not significant. The octahedral *M* site was first modelled with a mixed (Fe + Mn) scattering curve according to the chemical analysis (Tables 1 and 4); however, this did not improve the figure of merit of the refinement with respect to the site being fully populated by Fe. Six independent H sites were added to the structure model on the basis of the maxima found in the difference-Fourier map of the electron density. The relative O–H distances were restrained to a target value of 0.95 ± 0.03 Å. Convergence was achieved rapidly and the variance-covariance matrix showed no high correlation among the refined parameters; the six H sites were refined isotropically, with a restrained group value (Table 4). No peaks larger than +/– 0.5 e^{-} Å^{-3} were present in the final difference-Fourier maps of the electron density (Table 3). The final agreement index (R_1) was 0.0227 for 92 refined parameters and 1409 unique reflections with $F_o > 4\sigma(F_o)$ (Table 3). Atom coordinates and displacement parameters are reported in Table 4. Relevant bond lengths and angles are listed in Table 5.

Raman spectroscopy

The single-crystal Raman spectrum of albertiniite was collected using an Olympus BX40 microscope attached to a Jobin-Yvon Horiba LabRam confocal Raman spectrometer, equipped with CCD, at the University of Parma. The spectrum was collected by exciting the sample with a 473.1 nm laser light. The

TABLE 7 Comparison between the crystallographic features of albertiniite with gravegliaite and their synthetic analogues.

	Albertiniite	Synthetic α-$FeSO_3 \cdot 3H_2O$	Gravegliaite	Synthetic $MnSO_3 \cdot 3H_2O$
Reference	This work	[1]	[2]	[3]
Ideal formula	$Fe^{2+}(SO_3) \cdot 3H_2O$	$Fe^{2+}(SO_3) \cdot 3H_2O$	$Mn^{2+}(SO_3) \cdot 3H_2O$	$Mn^{2+}(SO_3) \cdot 3H_2O$
Crystal system	monoclinic	monoclinic	orthorhombic	orthorhombic
Space group	$P2_1/n$	$P2_1/n$	*Pnma*	*Pnma*
a (Å)	6.633(1)	6.604(2)	9.763(1)	9.72(2)
b (Å)	8.831(1)	8.693(1)	5.635(1)	5.63(1)
c (Å)	8.773(2)	8.714(2)	9.558(1)	9.53(2)
β (°)	96.106(8)	96.05(2)		
Z	4	4	4	4
Strongest X-ray lines	6.167 (14)	5.522 (m)	6.83(s)	
	5.533 (27)	4.661 (s)	4.33(vs)	
	5.257 (11)	3.878 (s)	3.43(vs)	
	4.998 (14)	3.277 (s)	2.704(m)	
	4.721 (100)	3.072 (m)	2.666(m)	
	4.353 (12)	2.863 (m)	2.414(m)	
	3.897 (12)	2.753 (m)	1.726(m)	
	3.539 (93)	2.220 (m)		
	3.290 (10)	1.939 (m)		
	2.830 (14)	1.870 (m)		
Density	2.469 (calc.)		2.39 (calc.)	2.40 (meas), 2.40 (calc)
Colour	Colourless, pale yellow, transparent	Pale green, transparent	Colourless, transparent	Colourless, transparent
Morphology	Prismatic		Prismatic {010}	Prismatic {010}

[1] Johansson and Lindquist (1979); [2] Basso *et al.* (1991); [3] Baggio and Baggio (1976). m = medium; s = strong; vs = very strong.

https://doi.org/10.1180/minmag.2016.080.033 Published online by Cambridge University Press

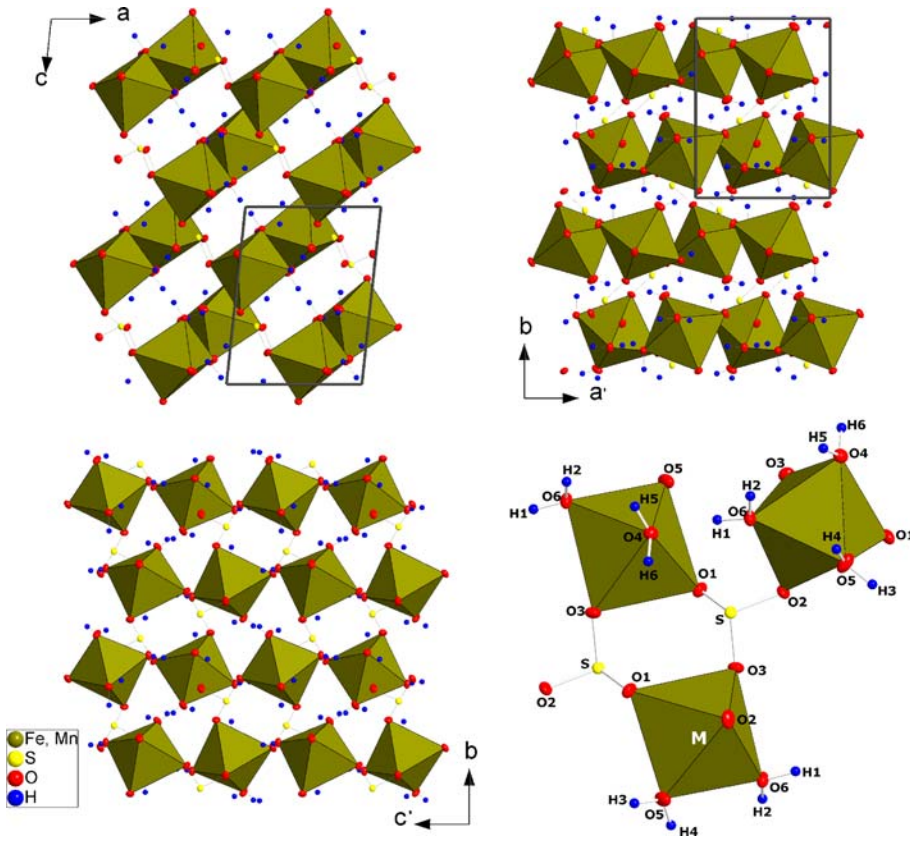

FIG. 5. The crystal structure of albertiniite based on the structure refinement of this study with 50% thermal ellipsoid probability factors.

laser beam was focused on the sample on a spot with nearly 2 μm diameter of (objective 50x) and the confocal aperture was set at 150 μm. The Raman spectrum was collected in back-scattered geometry, in the spectral range 100–4000 cm^{-1}, with 200 s counting time and three accumulations (Figs 3 and 4). The position of the Raman bands was measured using a Gauss-Lorentzian deconvolution procedure with the *LabSpec v.*5 software, with a precision of 0.5 cm^{-1}. The Raman bands are reported in Table 6.

Discussion

The new mineral albertiniite is the product of the intermediate oxidation of Fe sulfides (e.g. pyrite, arsenopyrite) in a Ca-rich hydrothermal environment. Albertiniite is a (Fe^{2+}, Mn)-sulfite trihydrate chemically related to gravegliaite, Strunz 4.JE.05, Dana 34.2.05.2. It corresponds to the monoclinic Fe equivalent of gravegliaite, ideally $Mn^{2+}(SO_3)\cdot 3H_2O$ (Basso *et al.*, 1991; Table 7). A comparison of the crystallographic features of albertiniite and those of its synthetic counterpart α-$FeSO_3\cdot 3H_2O$, gravegliaite and synthetic $MnSO_3\cdot 3H_2O$ is given in Table 7. Among these, the Mn-dominant minerals have orthorhombic structures (as observed in gravegliaite and synthetic $MnSO_3\cdot 3H_2O$), whereas the Fe-dominant albertiniite and α-$FeSO_3\cdot 3H_2O$ structures are monoclinic (Table 7). A view of the crystal structure of albertiniite is shown in Fig. 5. Each Fe atom is 6-coordinated to three different sulfite O atoms and three H_2O molecules, giving a slightly distorted octahedron (the difference between the longest and the shortest *M*–O distances is ~0.17 Å; Table 5). The sulfite group shows S–O bond distances similar to those reported previously for the synthetic α-$FeSO_3\cdot 3H_2O$, with S–O1 > S–O3 > S–O2 (Johansson and Lindqvist, 1979; Table 5).

https://doi.org/10.1180/minmag.2016.080.033 Published online by Cambridge University Press

Each sulfite ion is bonded to three Fe atoms, giving a three-dimensional net of Fe–O–S interactions. The H-bonding scheme in albertiniite is O1···H2–O6–H1···O4, O3···H4–O5–H3···O2 and O6···H6–O4-H5···O1 (Table 5). All the H-bonds show O–H···O angles > 160°and H···O distances ≤ 2 Å.

The Raman spectrum of albertiniite (Figs 3 and 4, Table 6) is typical of a hydrated sulfite, containing the stretching (i.e. 3215 and 3350 cm^{-1}, Table 6) and bending (i.e. 1660 cm^{-1}) modes of H_2O, along with stretching and bending modes of the pyramidal SO_3^{2-} ion (observed between 438 and 970 cm^{-1}). Free SO_3^{2-} is expected to show only four Raman modes, while in a crystal structure the local distortion will remove the double degeneracy of the asymmetric modes ν_3 and ν_4, leading to a total of six modes. Here we observe a total of 11 modes that can be ascribed to SO_3^{2-} (Table 6). For any given oxygen atom (O_j) belonging to the coordination environment of the octahedral site, the presence of Mn and Fe (co-sharing the *M* site) leads to slightly different *M*–O_j distances at the local scale, which, in turn, will give different S–O_j distances. We are inclined to consider the doubling of the Raman active modes of the SO_3^{2-} group as being due to local Fe/Mn ordering.

Acknowledgements

The authors are grateful to Claudio Albertini for having provided the new mineral used in this study. The authors are particularly grateful to P. Leverett, Jakub Plášil and an anonymous reviewer, and to the Editors P. Williams and S. Mills for their constructive comments.

References

Albertini, C., Bertolotti, G.P., Grassi, V., Gruppo Grotte Novara, Lana, E., Manni, C. and Montrasio, A. (2014) *Miniere e minerali del Vergante e Val d'Agogna* (Arona (VB), editor). Gruppo Archeologico, Storico, Mineralogico Aronese (G.A.S.M.A.), Italy.

Baggio, R.F. and Baggio, S. (1976) Chrystal structure and chemical bonding of manganese (II) sulphite trihydrate. *Acta Crystallographica*, **B32**, 1959–1962.

Basso, R., Lucchetti, G. and Palenzona, A. (1991) Gravegliaite, $MnSO_3 \cdot 3H_2O$, a new mineral from Val Graveglia (Northern Appennines, Italy). *Zeitschrift für Kristallographie*, **197**, 97–106.

Farrugia, L.J. (1999) WinGX suite for small-molecule single-crystal crystallography. *Journal of Applied Crystallography*, **32**, 837–838.

Graeser, S., Schwander, H., Demartin, F., Gramaccioli, C.M., Pilati, T. and Reusser, E. (1994) Fetiasite $(Fe^{2+},Fe^{3+},Ti)_3O_2[As_2O_5]$, a new arsenite mineral; its description and structure determination. *American Mineralogist*, **79**, 996–1002.

Hentschel, G., Tillmanns, E. and Hofmeister, W. (1985) Hannebachite, natural calciumsulfite hemihydrate, $CaS0_3.1/2H_2O$. *Neues Jahrbuch für Mineralogie Monatshefte*, **1985**, 241–250.

Johansson, L.G. and Lindquist, O. (1979) The crystal structure of iron (II) sulfite trihydrate, α-$FeSO_3 \cdot 3H_2O$. *Acta Crystallographica*, **B35**, 1017–1020.

Larson, A.C. (1967) Inclusion of secondary extinction in least-squares calculations. *Acta Crystallographica*, **23**, 664–665.

Laugier, J. and Bochu, B. (1999) *CELREF: Cell parameters refinement program from powder diffraction diagram.* Laboratoire des Matériaux et du Génie Physique, Ecole Nationale Supérieure de Physique de Grenoble (INPG), Grenoble, France.

Mandarino, J.A. (1981) The Gladstone-Dale relationship: Part IV. The compatibility concept and its application. *The Canadian Mineralogist*, **19**, 441–450.

Paar, W.H., Braithwaite, R.S.W., Chen, T.T. and Keller, P. (1984) A new mineral, scotlandite ($PbSO_3$) from Leadhills, Scotland; the first naturally occurring sulfite. *Mineralogical Magazine*, **48**, 283–288.

Sheldrick, G.M. (1997) *SHELX-97 – A program for crystal structure refinement.* University of Göttingen, Germany.

Sheldrick, G.M. (2008) A short history of SHELX. *Acta Crystallographica*, **A64**, 112–122.

Strunz, H. and Nickel, E.H. (2001) *Strunz Mineralogical Tables.* 9th Edition, E. Schweizerbart-Verlag, Stuttgart, Germany.

Vignola, P., Gatta, G.D., Rotiroti, N., Gentile, P., Hatert, F., Baijot, M., Bersani, D., Risplendente, A. and Pavese, A. (2015) Albertiniite, IMA 2015-004. CNMNC. Newsletter No. 25, June 2015, page 532; *Mineralogical Magazine*, **79**, 529–535.

Weidenthaler, C., Tillmanns, E. and Hentschel, G. (1993) Orschallite, $Ca_3(SO_3)_2SO_4$*$12H_2O$, a new calcium-sulfite-sulfate-hydrate mineral. *Mineralogy and Petrology*, **48**, 167–177.

Wilson, A.J.C. and Prince, E. (1999) *International Tables for Crystallography Vol. C, Mathematical, Physical and Chemical Tables.* 2nd edition. Kluwer, Dordrecht, The Netherlands.

https://doi.org/10.1180/minmag.2016.080.033 Published online by Cambridge University Press